

# Diverse Alkyl–Silyl Cross-Coupling via Homolysis of Unactivated C(sp<sup>3</sup>)–O Bonds with the Cooperation of Gold Nanoparticles and Amphoteric Zirconium Oxides

Hiroki Miura,\* Masafumi Doi, Yuki Yasui, Yosuke Masaki, Hidenori Nishio, and Tetsuya Shishido\*



Cite This: <https://doi.org/10.1021/jacs.2c12311>



Read Online

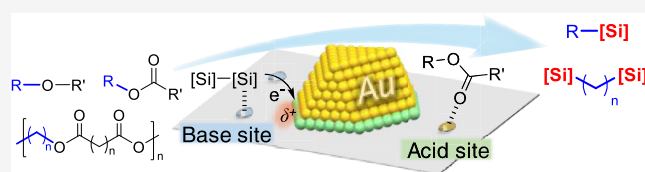
ACCESS |

Metrics & More

Article Recommendations

Supporting Information

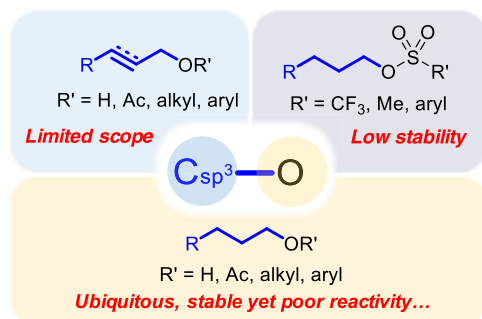
**ABSTRACT:** Since C(sp<sup>3</sup>)–O bonds are a ubiquitous chemical motif in both natural and artificial organic molecules, the universal transformation of C(sp<sup>3</sup>)–O bonds will be a key technology for achieving carbon neutrality. We report herein that gold nanoparticles supported on amphoteric metal oxides, namely, ZrO<sub>2</sub>, efficiently generated alkyl radicals via homolysis of unactivated C(sp<sup>3</sup>)–O bonds, which consequently promoted C(sp<sup>3</sup>)–Si bond formation to give diverse organosilicon compounds. A wide array of esters and ethers, which are either commercially available or easily synthesized from alcohols participated in the heterogeneous gold-catalyzed silylation by disilanes to give diverse alkyl-, allyl-, benzyl-, and allenyl silanes in high yields. In addition, this novel reaction technology for C(sp<sup>3</sup>)–O bond transformation could be applied to the upcycling of polyesters, i.e., the degradation of polyesters and the synthesis of organosilanes were realized concurrently by the unique catalysis of supported gold nanoparticles. Mechanistic studies corroborated the notion that the generation of alkyl radicals is involved in C(sp<sup>3</sup>)–Si coupling and the cooperation of gold and an acid–base pair on ZrO<sub>2</sub> is responsible for the homolysis of stable C(sp<sup>3</sup>)–O bonds. The high reusability and air tolerance of the heterogeneous gold catalysts as well as a simple, scalable, and green reaction system enabled the practical synthesis of diverse organosilicon compounds.



## 1. INTRODUCTION

Carbon–oxygen (C–O) bonds are a ubiquitous chemical motif that is found in both native and artificial organic

### Scheme 1. Reactivity of C(sp<sup>3</sup>)–O Bonds



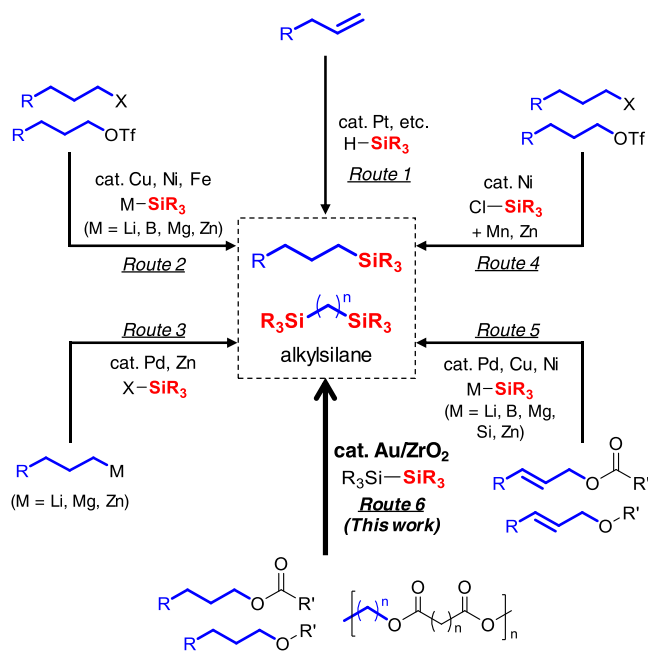
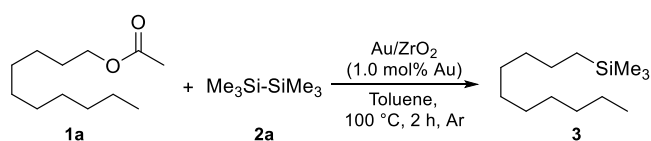
molecules. Especially, the C(sp<sup>3</sup>)–O bond is often found not only in oxygenated chemical feedstock, such as alcohols, ethers, and esters, but also in natural biomass compounds, such as lignin, cellulose, and hemicellulose, and functional polyesters. Accordingly, the universal transformation of abundant C(sp<sup>3</sup>)–O bonds should be a key technology for achieving carbon neutrality while rapidly upgrading chemical raw materials and diversifying molecular complexity as well as the degradation of chemical wastes.<sup>1</sup> Remarkable progress in bond

activation technology based on organic and organometallic chemistry over the past half-century has revealed several strategies for activating robust C(sp<sup>3</sup>)–O bonds (Scheme 1).<sup>2</sup> The use of allyl and propargyl compounds, i.e., the introduction of  $\pi$  moieties at the  $\beta$ - $\gamma$  C–C bond of alkyl groups, facilitates cleavage of C(sp<sup>3</sup>)–O bonds thanks to the interaction between Lewis acids and substrates or to the high stability of the resulting allyl and propargyl fragments.<sup>3</sup> Alternatively, connection with strong electron-withdrawing groups, such as sulfonyl groups, decreases the energy of C(sp<sup>3</sup>)–O bonds.<sup>4</sup> However, the general strategy for enabling alcohols, ethers, and stable esters, such as alkyl acetates, as a carbon electrophile to accommodate in cross-coupling reactions remains underdeveloped.<sup>5</sup>

Alkyl–silyl coupling to synthesize alkylsilanes is a typical example of the limitations of cross-coupling reactions (Scheme 2).<sup>6</sup> Alkylsilanes are important scaffolds in materials chemistry as well as intermediates in organic synthesis for synthesizing value-added molecules such as pharmaceuticals, agrochemicals, and functional materials.<sup>7</sup> Although the hydrosilylation of

Received: November 20, 2022

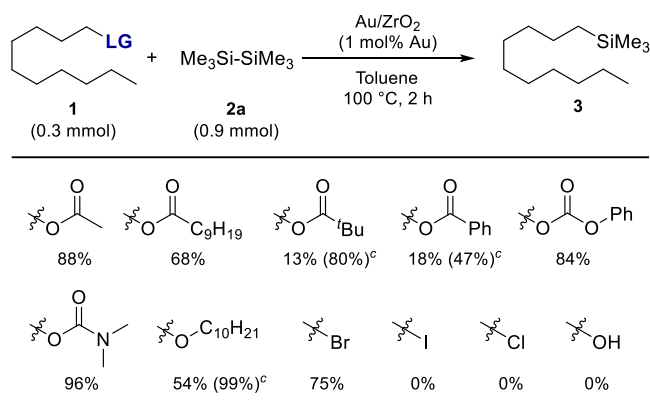
Scheme 2. Synthetic Route to Alkylsilanes

Table 1. Au/ZrO<sub>2</sub>-Catalyzed Silylation of C(sp<sup>3</sup>)-O Bonds<sup>a</sup>

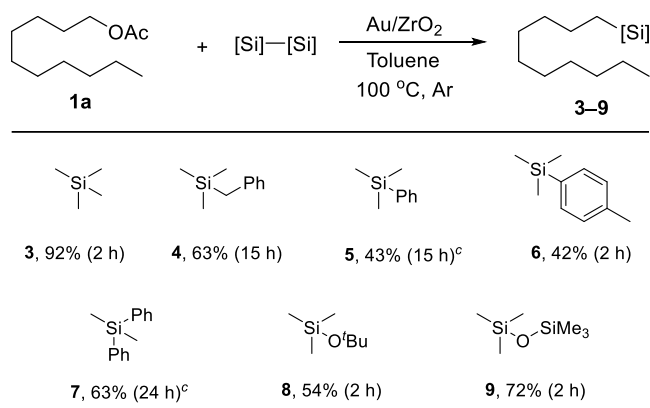
entry	variation from the standard condition	yield of 3 (%) <sup>b</sup>
1	none	88
2	Ni, Cu, Pd, Ag, or Pt instead of Au	0
3	1,4-dioxane instead of toluene	37
4	DMF or CH <sub>3</sub> CN instead of toluene	0
5	Al <sub>2</sub> O <sub>3</sub> instead of ZrO <sub>2</sub>	69
6	SiO <sub>2</sub> instead of ZrO <sub>2</sub>	12
7	TiO <sub>2</sub> instead of ZrO <sub>2</sub>	6
8	Nb <sub>2</sub> O <sub>5</sub> instead of ZrO <sub>2</sub>	0
9	Me <sub>2</sub> SAuCl instead of Au/ZrO <sub>2</sub>	0
10	ZrO <sub>2</sub> instead of Au/ZrO <sub>2</sub>	0
11	at 80 °C for 8 h	84
12	under open air	93
13	gram-scale reaction (5.0 mmol of 1a) for 8 h	84

<sup>a</sup>Reaction conditions: 1a (0.30 mmol), 2a (0.9 mmol), catalyst (1.0 mol % as metal), and toluene (1.0 mL) at 100 °C for 2 h. <sup>b</sup>Yields were determined by gas chromatography (GC) analysis using biphenyl as an internal standard.

alkenes is a well-established method for accessing alkylsilanes (Scheme 2, route 1),<sup>8</sup> the control of regioselectivity in the reaction of 1,2-disubstituted alkenes is still a significant challenge. Transition metal-catalyzed cross-coupling of an alkyl electrophile with a silyl-metal nucleophile has emerged as an alternative tool for the regioselective formation of C-Si bonds (Scheme 2, route 2).<sup>9</sup> In addition, alkyl metal reagents obtained via the umpolung reaction of alkyl halides are useful for the alkylation of silicon electrophiles under the influence of transition-metal catalysis (Scheme 2, route 3).<sup>10</sup> More recently, cross-electrophile coupling reactions by a Ni catalyst in the presence of a stoichiometric amount of a metallic reductant

Table 2. Silylation of a Series of Alkyl Electrophiles<sup>a,b</sup>

<sup>a</sup>Reaction conditions: 1 (0.30 mmol), 2a (0.9 mmol), Au/ZrO<sub>2</sub> (1.0 mol % as Au), and toluene (1.0 mL) at 100 °C for 2 h. <sup>b</sup>Yields were determined by GC analysis using biphenyl as an internal standard. <sup>c</sup>Reaction for 18 h.

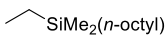
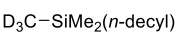
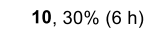
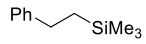
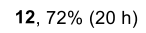
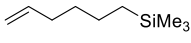
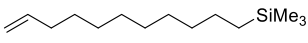
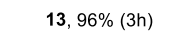
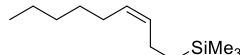
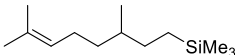
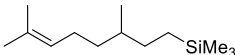
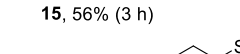
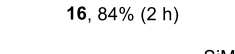
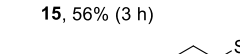
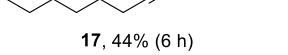
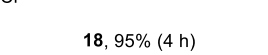
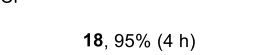
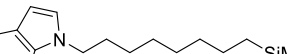
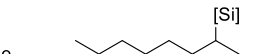
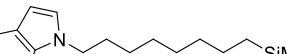
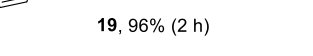
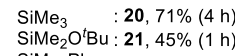
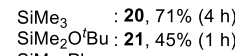

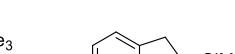

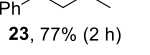
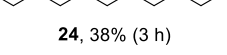
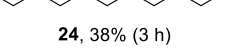
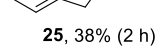
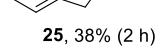
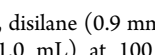
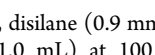
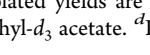
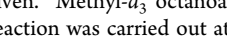
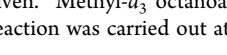
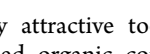
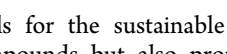
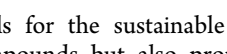
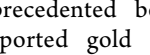
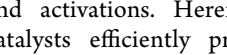
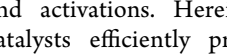
Table 3. Scope of Disilanes<sup>a,b</sup>

<sup>a</sup>Reaction conditions: 1a (0.30 mmol), disilane (0.9 mmol), Au/ZrO<sub>2</sub> (3.0 mol % as Au), and toluene (1.0 mL) at 100 °C. <sup>b</sup>Isolated yields are given. <sup>c</sup>Reaction was carried out at 130 °C in mesitylene.

have appeared efficient ways to synthesize alkylsilanes (Scheme 2, route 4).<sup>11</sup> However, metallic reagents and alkyl triflates suffer from instability against air, moisture, and high temperature, which hinders the use of such C-Si coupling as a convenient and scalable tool in both the laboratory and industrial settings. While transition metals catalyze silylation of allyl and propargyl esters to afford synthetically useful allylsilanes<sup>12</sup> and allenyl silanes<sup>13</sup> (Scheme 2, route 5), the development of a universal method that enables the formation of a variety of C(sp<sup>3</sup>)-Si bonds is still a significant challenge.

On the other hand, heterogeneous catalysts, especially supported metal catalysts, are widely used for manufacturing not only bulk chemicals but also fine chemicals in the chemical industry, thanks to their high stability and insolubility in organic and inorganic media.<sup>14</sup> For instance, supported gold nanoparticle catalysts have been reported to show excellent catalysis toward carbon-heteroatom bond formations.<sup>15</sup> Furthermore, recent studies on the cooperation between the redox properties of metal nanoparticles and the acid-base function of the support explored novel perspectives on supported catalysts toward selective molecular transformations.<sup>16</sup> The results imply that heterogeneous catalysts are not

Table 4. Scope of Alkyl Acetates<sup>a,b</sup>

$R_{\text{alkyl}}-\text{OAc}$	$[\text{Si}]-[\text{Si}]$	$\xrightarrow[\text{Toluene, 100 } ^\circ\text{C, Ar}]{\text{Au/ZrO}_2}$	$R_{\text{alkyl}}-[\text{Si}]$ 10–25
			 10, 30% (6 h)
			 12, 72% (20 h)
			 13, 96% (3 h)
			 14, 83% (4 h)
			 15, 56% (3 h)
			 16, 84% (2 h)
			 17, 44% (6 h)
			 18, 95% (4 h)
			 19, 96% (2 h)
			 20, 71% (4 h)
			 21, 45% (1 h)
			 22, 45% (24 h) <sup>d</sup>
			 23, 77% (2 h)
			 24, 38% (3 h)
			 25, 38% (2 h)

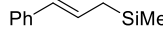
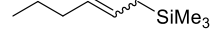
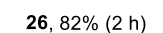



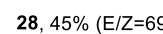

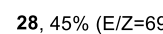

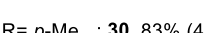
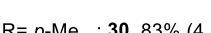
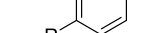
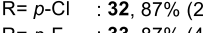
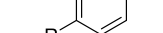



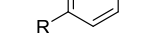
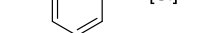
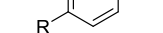
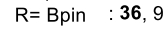
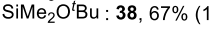
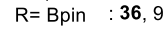
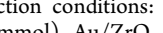
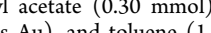
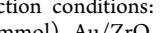



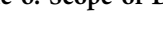

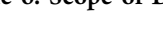

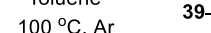

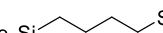
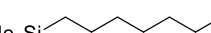
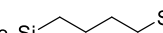
<sup>a</sup>Reaction conditions: alkyl acetate (0.30 mmol), disilane (0.9 mmol), Au/ZrO<sub>2</sub> (3.0 mol % as Au), and toluene (1.0 mL) at 100 °C. <sup>b</sup>Isolated yields are given. <sup>c</sup>Methyl-*d*<sub>3</sub> octanoate was used instead of methyl-*d*<sub>3</sub> acetate. <sup>d</sup>Reaction was carried out at 130 °C in mesitylene.

only attractive tools for the sustainable synthesis of value-added organic compounds but also promising materials for unprecedented bond activations. Herein, we report that supported gold catalysts efficiently promoted alkyl–silyl cross-coupling (Scheme 2, route 6). A series of esters and ethers bearing unactivated C(sp<sup>3</sup>)–O bonds underwent silylation by disilanes to give diverse alkyl-, allyl-, benzyl-, and allenyl silanes in high yields. Furthermore, the present Au-catalyzed silyl cross-coupling enabled the concurrent degradation of polyesters and the synthesis of organosilanes, i.e., upcycling of polyesters. Mechanistic studies corroborated that the generation of alkyl radicals is involved in C(sp<sup>3</sup>)–Si coupling and the cooperation of gold and an acid–base pair on amphoteric oxides is responsible for the homolysis of stable C(sp<sup>3</sup>)–O bonds for generating alkyl radicals, which consequently promote C(sp<sup>3</sup>)–Si bond formation to give diverse organosilicon compounds. The high reusability and air tolerance of the heterogeneous gold catalysts as well as the simple, scalable, and green reaction system enable the practical synthesis of diverse organosilicon compounds.

## 2. RESULTS AND DISCUSSION

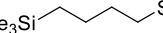
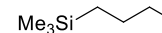
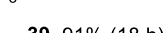








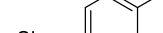
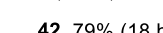








**2.1. Optimization of Catalysts and Reaction Conditions.** We initially examined the catalytic activity of a series of metal nanoparticles supported on ZrO<sub>2</sub> toward the cross-coupling of decyl acetate (1a) with hexamethyldisilane (2a) (Table 1). The reaction in toluene with 1.0 mol % of Au/ZrO<sub>2</sub>

Table 5. Scope of Allyl and Benzyl Acetates<sup>a,b</sup>

$R_{\text{allyl}}-\text{OAc}$	$[\text{Si}]-[\text{Si}]$	$\xrightarrow[\text{Toluene, 100 } ^\circ\text{C, Ar}]{\text{Au/ZrO}_2}$	$R_{\text{allyl}}-[\text{Si}]$ 26–29
			 26, 82% (2 h)
			 27, 67% (E/Z=70:30, 3 h)
			 28, 45% (E/Z=69:31, 3 h)
			 29, 59% (3 h)
			 30, 83% (4 h)
			 31, 89% (4 h)
			 32, 87% (2 h)
			 33, 87% (4 h)
			 34, 77% (2 h)
			 35, 83% (1 h)
			 36, 93% (2 h)
			 37, 53% (3 h)
			 38, 67% (1 h)

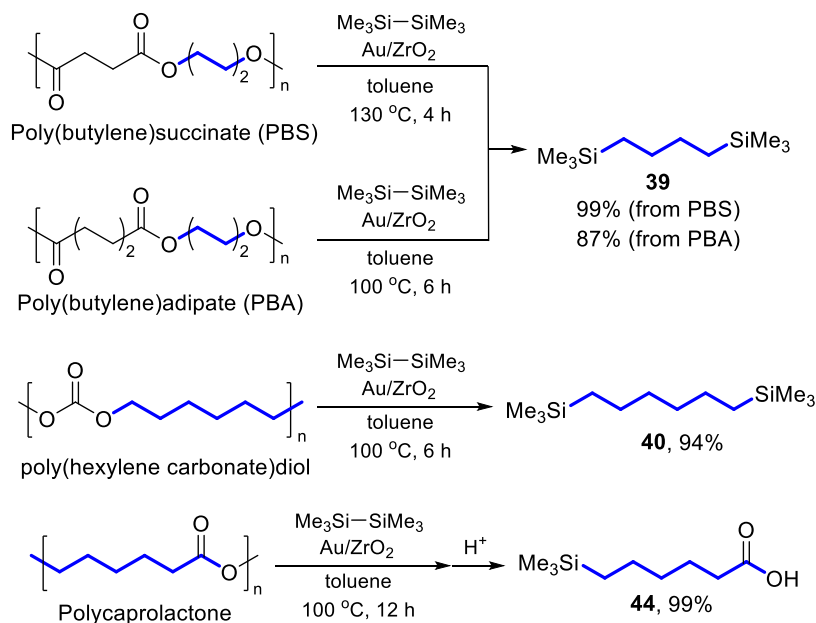
<sup>a</sup>Reaction conditions: allyl or benzyl acetate (0.30 mmol), disilane (0.9 mmol), Au/ZrO<sub>2</sub> (3.0 mol % as Au), and toluene (1.0 mL) at 100 °C. <sup>b</sup>Isolated yields are given.

Table 6. Scope of Diesters<sup>a,b</sup>

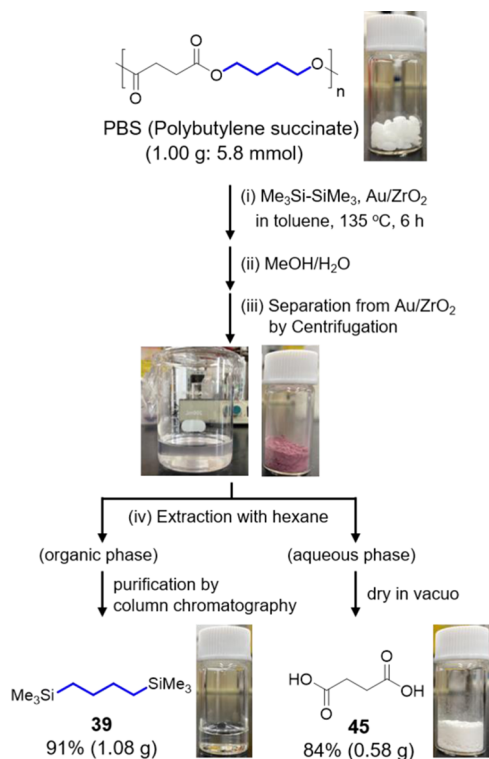
$\text{AcO}-R_{\text{alkyl}}-\text{OAc}$	$\text{Me}_3\text{Si}-\text{SiMe}_3$	$\xrightarrow[\text{Toluene, 100 } ^\circ\text{C, Ar}]{\text{Au/ZrO}_2}$	$[\text{Si}]-R_{\text{alkyl}}-[\text{Si}]$ 39–43
			 39, 91% (18 h)
			 40, 99% (18 h)
			 41, 99% (18 h)
			 42, 79% (18 h)
			 43, 69% (18 h)
			 n.d.
			 n.d.

<sup>a</sup>Reaction conditions: diacetate (0.30 mmol), 2a (0.9 mmol), Au/ZrO<sub>2</sub> (3.0 mol % as Au), and toluene (1.0 mL) at 100 °C. <sup>b</sup>Isolated yields are given.

## Scheme 3. Depolymerizative Silylation of Polyesters



## Scheme 4. Procedure for Gram-Scale Depolymerizative Silylation of PBS



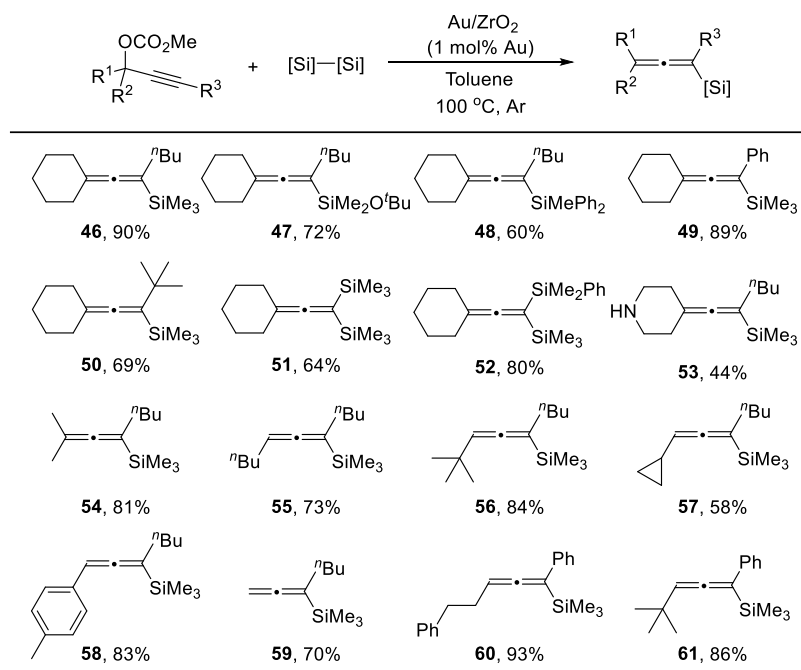
catalyst at  $100\text{ }^{\circ}\text{C}$  gave the corresponding alkylsilane (**3**) in 88% yield (entry 1). In contrast, the replacement of Au with Ni, Cu, Pd, and Pt resulted in no conversion of **1a** (entry 2). Toluene was found to be the solvent of choice, whereas the reaction rate was greatly reduced with the use of 1,4-dioxane, dimethylformamide (DMF), and acetonitrile (entries 3 and 4). The supporting materials for Au nanoparticles had a dramatic impact on their catalytic activity. In sharp contrast to the comparable catalytic activities of  $\text{Au/Al}_2\text{O}_3$  and  $\text{Au/ZrO}_2$ , the use of  $\text{SiO}_2$ ,  $\text{TiO}_2$ , or  $\text{Nb}_2\text{O}_5$ -supported catalysts showed a

quite low activity (entries 5–8). Cationic Au complexes, which are often used as catalysts for organic synthesis, and  $\text{ZrO}_2$  alone showed no activity for the title reaction (entries 9 and 10), which indicates that Au NPs were indispensable for promoting  $\text{C}(\text{sp}^3)\text{-Si}$  coupling. While a prolonged reaction period was required, **3** was obtained in high yield even at  $80\text{ }^{\circ}\text{C}$  (entry 11). Notably,  $\text{Au/ZrO}_2$  still showed remarkable catalytic performance under air in sharp contrast to previous  $\text{C}(\text{sp}^3)\text{-Si}$  coupling with the use of organometallic reagents, which suffers in the presence of air or moisture (entry 12). Thanks to this robustness of  $\text{Au/ZrO}_2$ , the reaction of 5 mmol of **1a** gave alkylsilane **3** at a gram scale (1.08 g, 84%, entry 13).

**2.2. Effect of Leaving Groups.** An array of leaving groups of alkyl electrophiles were acceptable for  $\text{C}(\text{sp}^3)\text{-Si}$  coupling by  $\text{Au/ZrO}_2$  catalysts (Table 2). Along with acetate, carboxylate with a long alkyl chain, namely, decanoate, could be used as a good leaving group. In contrast, bulky  $t\text{Bu}$  and Ph groups significantly impeded the reaction, which implies that steric hindrance around the carbonyl functionality is a factor for dominating the reaction rates (vide infra). Conversely, phenyl carbonate and dimethyl carbamate were found to be good leaving groups to furnish **3**. Notably, silylation occurred selectively at  $\text{sp}^3$  carbon in the reaction of decyl phenyl carbonate, which suggests that supported Au catalysts were inert for the silylation of  $\text{C}(\text{sp}^2)\text{-O}$  bonds. We were delighted to find that the Au catalyst allowed alkyl ether to act as an alkyl electrophile in  $\text{C-Si}$  coupling to afford **3**. Additionally, we evaluated the possibility of alkyl halides as a carbon electrophile and found that only alkyl bromide underwent silylation to provide **3**. Although a direct conversion of  $\text{C-OH}$  bonds is an ideal cross-coupling, the reaction of decanol delivered a silyl group not at carbon but rather at oxygen to give silyl ether. This also indicates that a trimethylsiloxy group is not a suitable leaving group for Au-catalyzed  $\text{C-Si}$  coupling.

**2.3. Reaction Scope: Alkyl Esters to Alkylsilanes.** With the optimized reaction conditions and catalysts in hand, we next explored the scope of the Au-catalyzed  $\text{C-Si}$  coupling reaction. The coupling of decyl acetate with a wide variety of disilanes bearing different substituents proceeded smoothly to



Table 7. Synthesis of Allenyl Silanes over the Au/ZrO<sub>2</sub> Catalyst<sup>a,b</sup>

<sup>a</sup>Reaction conditions: propargyl carbonate (0.50 mmol), disilane (1.5 mmol), Au/ZrO<sub>2</sub> (1.0 mol % as Au), and toluene (1.0 mL) at 100 °C for 1 h.

<sup>b</sup>Isolated yields are given.

give structurally diverse alkylsilanes (Table 3). As in the previous metal-catalyzed C(sp<sup>3</sup>)-Si coupling, alkyl and aryl moieties were compatible with silyl groups to give the corresponding alkylsilanes (3–7). While substrates bearing Si–O bonds have hardly been used for C(sp<sup>3</sup>)-Si coupling, Au catalysts promoted the reaction of disilanes bearing alkoxy and siloxy groups to give the corresponding alkylsilanes (8 and 9).

Next, the scope of alkyl acetate was investigated (Table 4). Although hydrosilylation requires the use of gaseous olefins in the case of the introduction of short alkyl chains, such as methyl and ethyl groups, the present Au catalyst delivered ethyl and trideuteriomethyl groups at silyl groups (10 and 11) with the use of easily handled liquid esters. Evaluation of functional group tolerance during the Au-catalyzed C–Si coupling revealed that internal and terminal alkene, alkyne, chloro, and amino moieties were compatible with the corresponding alkylsilanes (12–19). C(sp<sup>3</sup>)-Si bond formation also occurred at a secondary carbon to furnish alkylsilanes (20–25) bearing a branched alkyl chain.

Table 5 shows the scope of allyl and benzyl acetates. The reaction of allylic acetates also took place to give allylsilanes (26–29) in good to high yields. Various functional groups at an aromatic ring were tolerated during silylation at a benzylic carbon (30–34). Although a C(sp<sup>3</sup>)-O bond underwent silylation with a Au catalyst, C(sp<sup>2</sup>)-O and C(sp<sup>2</sup>)-B bonds remained intact (35 and 36). Introduction of an alkoxy-silyl moiety by C(sp<sup>3</sup>)-Si coupling has scarcely been explored, whereas the present Au catalyst gratifyingly provided the corresponding alkoxy-silanes (38).

Additionally, diesters derived from  $\alpha,\omega$ -alkanediols underwent silylation at both C–O bonds to furnish the corresponding bis(silyl)alkanes (39–43) in excellent yields (Table 6). Unfortunately, the reaction of vicinal diacetates resulted in no formation of disilylalkanes.

**2.4. Reaction Scope: Depolymerizative Silylation of Polyesters.** The fact that the supported Au catalysts were effective for the transformation of various C(sp<sup>3</sup>)-O bonds in alkyl esters into C–Si bonds allowed us to devise a depolymerizative silylation of polyesters. Since the accumulation of waste plastics is recognized as a serious modern environmental issue,<sup>17</sup> considerable attention has been focused on the discovery of novel methods for the degradation of plastics.<sup>18</sup> Even though the hydrolysis of polyesters by the use of a stoichiometric amount of strong base can deconstruct their robust structure into monomers,<sup>19</sup> this process provides only the starting substances, namely, diols and dicarboxylic acids. Furthermore, neutralization of alkali salts into carboxylic acids by acids has a considerable negative impact on the environment and reaction facility. Although hydrogenolysis of C<sub>acyl</sub>-O bonds in esters under the influence of transition metals is an alternative way for the decomposition of polyesters,<sup>20</sup> the reactions under harsh conditions cause excessive reduction of carboxylic acids to alcohols. Accordingly, the development of a catalytic process that can realize the depolymerizative transformation of polyesters into value-added chemicals under neutral and mild conditions provides a novel carbon circular pathway. Gratifyingly, the supported Au catalyst successfully promoted depolymerizative silylation of polyesters to give disilylalkanes without the use of basic additives (Scheme 3). For instance, the reaction of poly(1,4-butylene) succinate (PBS; 0.30 mmol per diol unit) with 2a (2.5 equiv with respect to C(sp<sup>3</sup>)-O bonds) in the presence of Au/ZrO<sub>2</sub> at 130 °C efficiently proceeded to furnish 0.29 mmol of 39 (99% yield based on diol). Furthermore, this process accompanied the quantitative formation of bis(trimethylsilyl) succinate, which undergoes hydrolysis to give succinic acid just by the addition of a protic solvent, such as water or methanol. This reaction can also be applied to the depolymerizative silylation of poly(1,4-butylene) adipate (PBA) to 39 and adipic acid.

Table 8. Alkyl Ethers to Alkylsilanes<sup>a</sup>

$\text{R-O-R} + [\text{Si}]-[\text{Si}] \xrightarrow[\text{100 } ^\circ\text{C, Ar}]{\text{Au/ZrO}_2 \text{ (3 mol\% Au) Toluene}} \text{R-[Si]} + [\text{Si}]\text{O-R}$			
Entry	Substrate	Product	Yield (%) <sup>b</sup>
1	$\text{C}_8\text{H}_{17}\text{-O-C}_8\text{H}_{17}$	$\text{C}_8\text{H}_{17}\text{-SiMe}_3$ <b>62</b>	98
2		$\text{Me}_3\text{Si-CH}_2\text{-CH}_2\text{-CH}_2\text{-CH}_2\text{-X}$ <b>63</b> , X=Cl	82
3		<b>64</b> , X=Br	46 <sup>c</sup>
4		<b>65</b> , X=OAc	95
5		<b>66</b> , X=CN	11
6		$(^t\text{BuO})\text{Me}_2\text{Si-CH}_2\text{-CH}_2\text{-CH}_2\text{-CH}_2\text{-OAc}$ <b>67</b>	31
7		$\text{Me}_3\text{Si-CH}_2\text{-CH}_2\text{-CH}_2\text{-CH}_2\text{-COOH}$ <b>68</b>	90
8		$\text{Me}_3\text{Si-CH}_2\text{-CH}_2\text{-CH}_2\text{-CH}_2\text{-O-Ph}$ <b>69</b>	79
9		$\text{Me}_3\text{Si-CH}_2\text{-CH}_2\text{-CH}_2\text{-CH}_2\text{-OH}$ <b>70</b>	0
10		$\text{Me}_3\text{Si-CH}_2\text{-CH}_2\text{-CH}_2\text{-CH}_2\text{-CH}_2\text{-Cl}$ <b>70</b>	83
11		$\text{Me}_3\text{Si-CH}_2\text{-CH}_2\text{-CH}_2\text{-CH}_2\text{-CH}_2\text{-OH}$ <b>71</b>	81
12		$\text{Me}_3\text{Si-CH}_2\text{-CH}_2\text{-CH}_2\text{-CH}_2\text{-CH}_2\text{-N(Ph)-CH}_2\text{-OH}$ <b>72</b>	80
13		$\text{Me}_3\text{Si-CH}_2\text{-CH}_2\text{-CH}_2\text{-CH}_2\text{-CHO}$ <b>73</b>	81
14		$(^t\text{BuOMe})_2\text{Si-CH}_2\text{-CH}_2\text{-CH}_2\text{-CH}_2\text{-CH}_2\text{-OSiMe}_2(^t\text{Bu})$ <b>74</b>	78

<sup>a</sup>Reaction conditions: ether (0.3 mmol), disilane (0.9 mmol), Au/ZrO<sub>2</sub> (3 mol % as Au), and toluene (1.0 mL) 100 °C under Ar.  
<sup>b</sup>Isolated yields are given. <sup>c</sup>Product was isolated as an alcohol.

Moreover, poly(hexylene carbonate) diol underwent C–O bond cleavage at 100 °C to afford bis(silyl)hexane **40** quantitatively. C–O bonds in polycaprolactone were also smoothly converted to C–Si bonds, and subsequent protonation of a silyl ester moiety finally gave an alkylsilane with carboxylic acid on an opposite side (**44**) as a sole product.

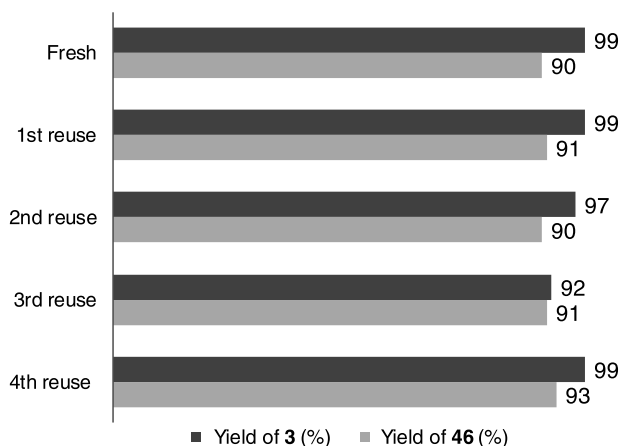
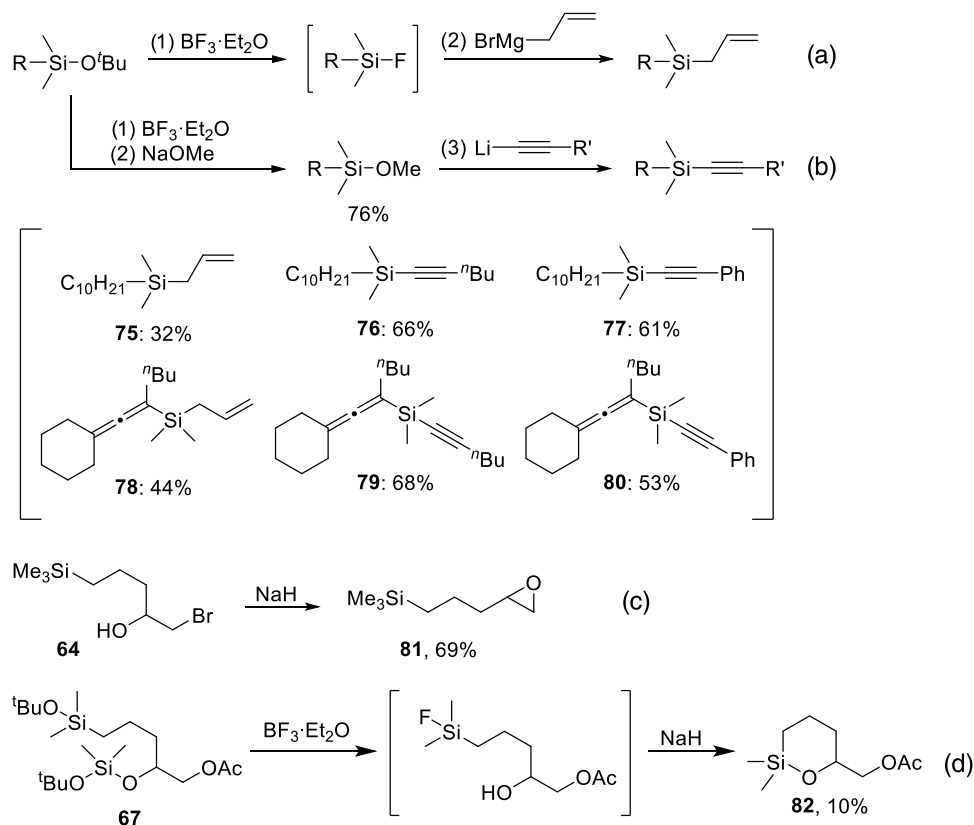
To evaluate the practicality of the system based on a supported Au catalyst, depolymerizative silylation of PBS was performed under gram-scale conditions (Scheme 4). After all of the C(sp<sup>3</sup>)–O bonds of PBS were consumed as determined by <sup>1</sup>H NMR, methanol was added to the reaction mixture for the desilylation of bis(trimethylsilyl)succinate. Extraction of the resulting reaction mixture with hexane and water transferred bis(silyl)alkane **39** and succinic acid **45** into the organic and aqueous phase, respectively. Drying and/or purification by column chromatography isolated both monomers in high yields. Consequently, this simple operation and the fact that atomic absorption spectroscopy revealed that there was no leaching of Au species into the reaction mixture

surely proved that the Au-catalyzed upcycling of polyesters can be performed in a practical manner.

**2.5. Reaction Scope: Propargyl Esters to Allenyl Silanes.** We next turned our attention to the cross-coupling of propargyl esters with disilanes to access allenyl silanes. The reactions of propargyl electrophiles with silicon nucleophiles, such as silylboranes and silylzinc, have been demonstrated under the influence of Cu and Rh catalysts,<sup>13</sup> whereas broadening of the substrate scope is still desirable due to the limited scope of substituents at silicon and the alkyne terminus. In this regard, Au/ZrO<sub>2</sub> efficiently delivered various silyl groups at an allene scaffold via the coupling of propargyl carbonates with disilanes as silyl nucleophiles (Table 7). Trimethylsilyl, dimethyl-*tert*-butoxysilyl, and diphenylmethylsilyl groups were compatible with the corresponding allene derivatives (**46–48**). In the Cu- and Rh-catalyzed synthesis of allenyl silanes, bulky substituents on the alkyne terminus hindered silylation at the γ-position probably because their reaction pathways involve the insertion of metal-boryl species into the alkyne moiety.<sup>13b,d</sup> In contrast, the Au-catalyzed reaction allowed aryl, *tert*-butyl, trimethylsilyl, and dimethylphenylsilyl groups to be acceptable as substituents for allenyl silanes (**49–52**). Besides, the Au/ZrO<sub>2</sub> catalyst enabled the synthesis of a wide array of allenyl silanes bearing the aryl and alkyl groups (**53–61**) via C–Si coupling of secondary and tertiary propargyl esters and disilanes.

**2.6. Reaction Scope: Alkyl Ethers to Alkylsilanes.** As shown in Table 2, the Au catalyst enabled the cross-coupling of dialkyl ether and disilane to furnish alkylsilane, which to the best of our knowledge, is the first example of the use of acyclic alkyl ethers as alkyl electrophiles for the synthesis of organosilanes.<sup>21</sup> Since ether functionalities are often found especially in molecules derived from cellulose and hemicellulose, upgrading of these compounds is quite important for carbon circular society. Therefore, we investigated the scope of silylation of alkyl ethers (Table 8). The C(sp<sup>3</sup>)–O bond of an acyclic symmetrical alkyl ether was readily transformed into C(sp<sup>3</sup>)–Si and O–Si bonds, thus providing the corresponding alkylsilane **62** in 98% yields. The ring-opening silylation of tetrahydrofuran bearing substituents at a C2 carbon took place predominantly at a CH<sub>2</sub>–O bond to furnish linear alkylsilanes with a functional group on an opposite side (**63–66**). Meanwhile, various functional groups were tolerated during C(sp<sup>3</sup>)–Si bond formation. For instance, halomethyl tetrahydrofuran afforded alkylsilanes with a haloalcohol moiety (**63** and **64**), which are readily transformed into epoxides (Scheme 5c). As with the reaction of alkyl ester, disilane with a Si–O bond could be used in the ring-opening silylation of a cyclic ether to give **67**. In addition, 2-tetrahydrofuroic acid was converted to a lactic acid bearing a silylalkyl group **68** in excellent yield. Selective cleavage of a C(sp<sup>3</sup>)–O bond occurred in the reaction of dihydrobenzofuran to give **69**. On the other hand, a cyclic ether with a tertiary alkyl group resulted in no formation of alkylsilane. Six-membered cyclic ethers, namely, tetrahydropyran and morpholine, could also be used as alkyl electrophiles to give the corresponding alkylsilanes with halogen, acetoxo, and amino functionalities (**70–72**). The coupling of dihydropyran with **2a** afforded alkane bearing silyl and silyl enol ether groups both at its terminus, whereas hydrolytic Si–O cleavage during purification through column chromatography gave silyl alkanal **73** as a final product. In contrast, silylation by a *bis-tert*-butoxy disilane provided a stable silyl enol ether **74** in 78% yield.

## Scheme 5. Synthetic Application of Alkylsilanes



Reaction conditions : alkyl acetate or propargyl carbonate (0.5 mmol), **2a** (1.5 mmol), Au/ZrO<sub>2</sub> (3.0 or 1.0 mol%), toluene (2.0 mL), 100 °C, 2 h, Yields were determined by GC.

Figure 1. Reusability of Au/ZrO<sub>2</sub> catalyst for C–Si bond formation.

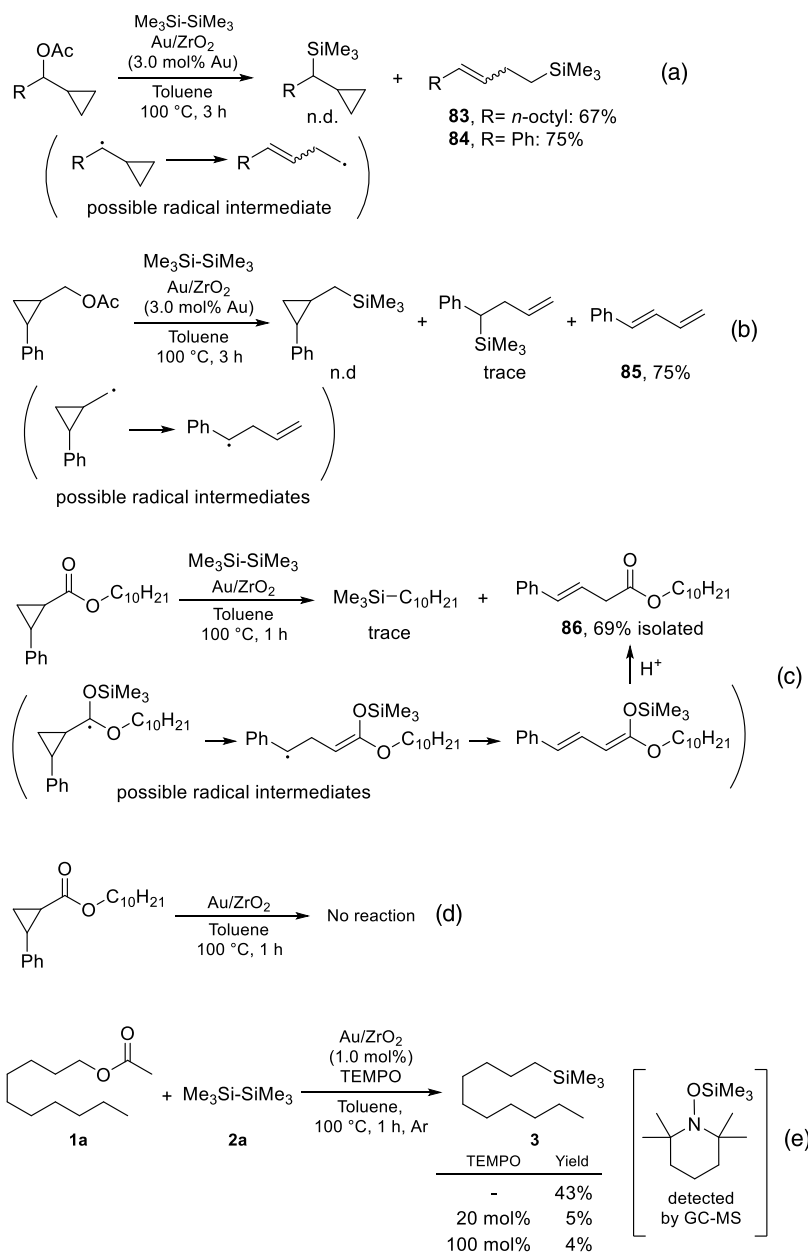
**2.7. Synthetic Application.** Subsequently, we explored the derivatization of organosilanes, which are synthesized by the Au-catalyzed silylation of C(sp<sup>3</sup>)–O bonds, into value-added molecules (Scheme 5). As demonstrated above, the present Au catalytic system enables the synthesis of alkyl and allenyl *tert*-butoxysilanes. Si–O<sup>t</sup>Bu was converted into Si–F by treatment with BF<sub>3</sub>·Et<sub>2</sub>O, and subsequent nucleophilic allylation provided allylsilanes **75** and **78** (Scheme 5a). Moreover, the treatment of BF<sub>3</sub>·Et<sub>2</sub>O and sodium methoxide transformed Si–O<sup>t</sup>Bu into Si–OMe, which underwent alkynylation to furnish alkynylsilanes (**76**, **77**, **79**, and **80**)

(Scheme 5b). Alkylsilane **64** with a 1,2-bromo alcohol moiety, which is obtained via ring-opening silylation of a tetrahydrofuran derivative, underwent a base-mediated ring-closing reaction to afford alkylsilane bearing an epoxy group **81** (Scheme 5c). The treatment of **67** with BF<sub>3</sub>·Et<sub>2</sub>O and NaH gave a six-membered silyl ether **82** (Scheme 5d).

**2.8. Reusability of the Au/ZrO<sub>2</sub> Catalyst.** Another significant characteristic of heterogeneous Au catalysts is their reusability, which is potentially superior to those of homogeneous catalysts. No significant decreases in product yields were observed in four consecutive catalytic runs for the cross-coupling of **2a** with both alkyl acetate and propargyl carbonate (Figure 1). Furthermore, hot filtration of the solid Au catalyst completely retarded further progress of the reaction (Supporting Information Figure S3), clearly indicating that the reaction system satisfies the essential requirements for realizing the sustainable and practical synthesis of organosilicon compounds.

**2.9. Mechanistic Studies.** We next turned our attention into the elucidation of the reaction mechanism as well as the effects of Au nanoparticles and the support. The cross-coupling of **2a** with secondary alkyl acetates bearing a cyclopropyl moiety at the  $\alpha$ -position gave homoallylic silanes **83** and **84** in high yields (Scheme 6a). Although a secondary alkylsilane was not obtained, similar ring-opening took place to give a diene **85** in the reaction of primary cyclopropylmethyl acetates (Scheme 6b). These findings indicate that C–Si cross-coupling includes the formation of a cyclopropylmethyl radical intermediate via the homolysis of C(sp<sup>3</sup>)–O bonds. Furthermore, the reaction of **2a** with alkyl cyclopropane carboxylate caused ring-opening of cyclopropyl group to give **86** as a sole product, which allows us to deduce that a silyl

## Scheme 6. Mechanistic Studies

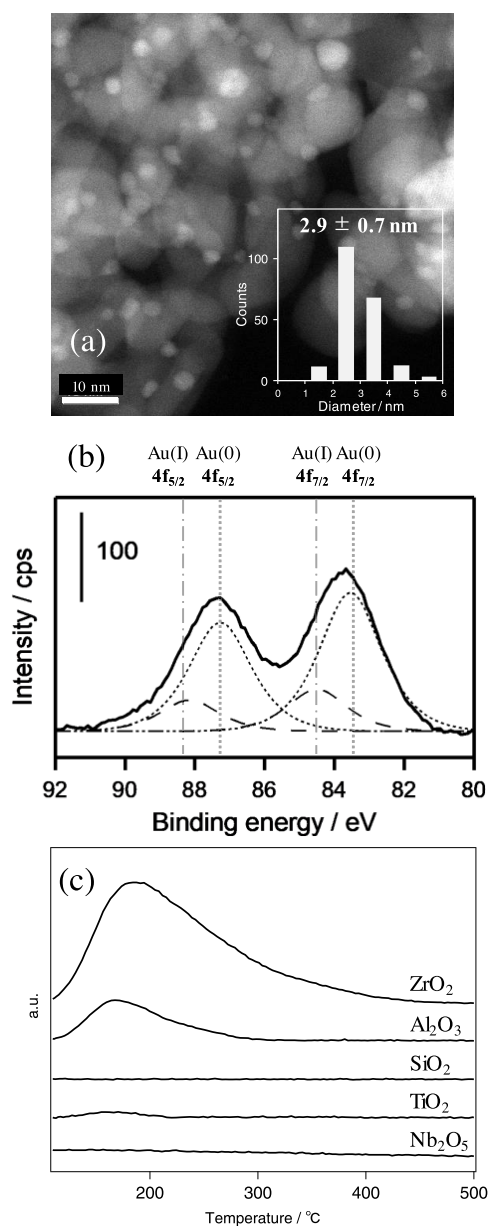


acetal radical was formed by the addition of a silyl radical to ester (Scheme 6c). In contrast, the cyclopropane structure was maintained when the reaction with Au/ZrO<sub>2</sub> was carried out in the absence of 2a, unambiguously proving that disilanes functioned as a source of silyl radical or single electron to generate an alkyl radical intermediate (Scheme 6d). Furthermore, a radical trap experiment using 2,2,6,6-tetramethylpiperidine 1-oxyl radical (TEMPO) significantly impeded the progress of the alkyl–silyl coupling, and silylated TEMPO was detected by gas chromatography–mass spectrometry (GC–MS) analysis (Scheme 6e). This result supports the generation of silyl radicals.

On the other hand, Studer and co-workers reported that nucleophilic silyl radicals were generated via single-electron oxidation of disilanes by Ir-based photo-redox catalysts under visible light irradiation.<sup>22</sup> Even though Au has a thermodynamically stable metallic state, cationic Au species with a high

oxidation potential ( $E^{\text{Au(0)/Au(I)}} = +1.69 \text{ V vs SHE}$ )<sup>23</sup> are known to form at the interface between their nanoparticles and metal oxides.<sup>24</sup> As shown in the high-angle annular dark-field scanning transmission electron microscopy (HAADF-STEM) image of Au/ZrO<sub>2</sub> in Figure 2a, the Au nanoparticles are highly dispersed at the surface of ZrO<sub>2</sub> with a mean diameter of 2.9 nm. Furthermore, a curve-fitting analysis of the X-ray photoelectron (XP) spectrum of Au/ZrO<sub>2</sub> before the catalytic reaction revealed the presence of a non-negligible amount of Au(I) species (ca. 20% in all surface Au species) at the surface of the catalyst (Figure 2b). However, no remarkable difference of the Au(I)/Au(0) ratios was ascertained among the supported Au catalysts tested (Figure S12), which indicates that the Au(I)/Au(0) ratio is not a dominant factor for the catalytic activity. While the oxidation potential of hexamethyldisilane 2a ( $E^{1/2} = +1.71 \text{ V vs SHE}$ ) was almost similar to that of Au(I) species, the fact that the oxidation potential of





**Figure 2.** (a) HAADF-STEM image of Au/ZrO<sub>2</sub> and Au particle size distribution; (b) XP spectra of Au/ZrO<sub>2</sub>; and (c) CO<sub>2</sub>-TPD profiles of supported Au catalysts.

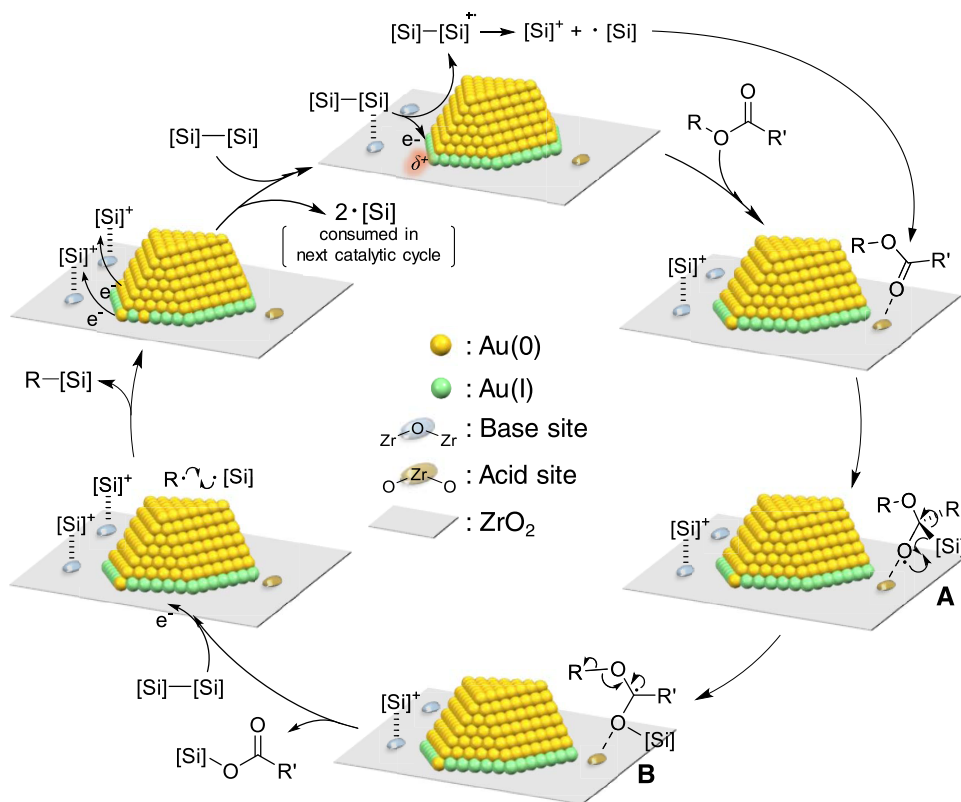
disilane can be reduced by the assistance of bases<sup>22</sup> turned our attention to the positive effect of an amphoteric oxide support on the activation of disilanes. An evaluation of basicity based on CO<sub>2</sub>-temperature programmed desorption (CO<sub>2</sub>-TPD) revealed that significant desorption bands appeared in the TPD profiles of ZrO<sub>2</sub> and Al<sub>2</sub>O<sub>3</sub>, whereas low-reactive SiO<sub>2</sub>, TiO<sub>2</sub>, and Nb<sub>2</sub>O<sub>5</sub> had scarce basicity (Figure 2c). This suggests that the basic nature of ZrO<sub>2</sub> and Al<sub>2</sub>O<sub>3</sub> facilitates the generation of disilane cation radicals via the single-electron transfer of disilanes to cationic Au. On the other hand, the reaction orders with respect to alkyl acetate and disilane were 1.1 and 0.1, which forces us to anticipate that the catalytic cycle includes the activation of alkyl acetates by the catalyst. Accordingly, we deduce that the activation of acetate by a Lewis acid site of amphoteric oxides facilitates the addition of nucleophilic silyl radicals to form silyl acetal radicals.<sup>25</sup> As shown in Table 2, the fact that steric hindrance at around the carbonyl moiety

impeded the formation of alkylsilanes implies that the nucleophilic attack of silyl radical is favored to occur at electrophilic carbon.

Based on these mechanistic investigations, we propose the possible reaction mechanism of alkyl–silyl cross-coupling over Au catalysts supported on amphoteric oxides in Scheme 7. Bridging oxygen between metal elements (M–O–M) is generally accepted as a basic site at the surface of metal oxides. Hence, disilane adsorbs initially at a Lewis basic site of the support, which triggers single-electron transfer from disilane to Au NPs to form its cation radical. Subsequently, the fragmentation of Si–Si bond occurs to generate silyl radicals. The resulting silyl cation would be trapped at the basic site of metal oxides. Although the bulkiness at around a carbonyl group remarkably retarded the reaction (Table 2), the activation of alkyl esters by a Lewis acidic site of the support facilitated the attack of a silyl radical to form hemiacetal radical A. After 1,2 radical Brook rearrangement of A affords silyl acetal radical B, homolysis of a C(sp<sup>3</sup>)–O bond gives an alkyl radical with liberation of silyl acetate.<sup>26</sup> Recently, the MacMillan group reported similar homolysis of C(sp<sup>3</sup>)–O bonds of an amino acetal radical which is generated via single-electron oxidation by a photo-excited Ir complex.<sup>5b</sup> On the other hand, the reaction of unsymmetrical disilane and a cyclic ester, namely,  $\epsilon$ -caprolactone, gave four different products (Scheme S3 in the Supporting Information). Furthermore, the same reaction outcome was obtained in the coupling of two different symmetrical disilanes with the cyclic ether (Scheme S4). These control experiments unambiguously suggest that two disilane molecules participate in the present reaction to form alkylsilanes. Thus, the alkyl radical finally couples with another silyl radical formed from the second disilane to give alkylsilane. The resulting two silyl cations are probably reduced by two electrons abstracted by Au NPs from disilane to generate silyl radicals, which are consumed in another catalytic cycle. Thus, efficient silylation proceeds on the supported gold catalyst, the key to which is the proximity of the acid–base site to the Au NPs causing efficient single-electron oxidation of disilane and electrophilic activation of alkyl acetate on the solid surface. The addition of 4-dimethylaminopyridine (DMAP) or Y(OTf)<sub>3</sub> as an external base or acid to the reaction with Au/ZrO<sub>2</sub> remarkably inhibited the reaction (Scheme S5), which is probably because DMAP or Y(OTf)<sub>3</sub> deactivated the acid or base sites over ZrO<sub>2</sub>. This strongly suggests that the use of amphoteric oxides which possess fixed acid–base sites on their surface is essential for the reaction to proceed.

### 3. CONCLUSIONS

Diverse and practical C(sp<sup>3</sup>)–Si coupling by amphoteric oxide-supported Au catalysts was described. A variety of alkyl esters and ethers participated in the heterogeneous Au-catalyzed cross-coupling to give the corresponding alkyl, allyl, benzyl, and allenyl silanes. Furthermore, the present C(sp<sup>3</sup>)–O bond activation technology was successfully applied to upcycling of various polyesters, i.e., Au/ZrO<sub>2</sub> catalyst-enabled depolymerizative silylation of PBS to give disilyl butane and succinic acid in excellent yields. Mechanistic studies corroborated that the homolysis of stable C(sp<sup>3</sup>)–O bonds of alkyl esters proceeded to generate alkyl radicals. The cooperation of Au nanoparticles and the amphoteric nature of the support are responsible for the generation of silyl radicals and subsequent formation of alkyl radicals, thereby enabling efficient alkyl–silyl coupling to furnish diverse alkylsilanes. Several important

Scheme 7. Possible Reaction Mechanism for Alkyl–Silyl Cross-Coupling by Au/ZrO<sub>2</sub>

sustainable features of supported Au catalysts, such as high reusability and air tolerance of the heterogeneous gold catalysts as well as the simple and scalable reaction system, enable the practical synthesis of diverse organosilicon compounds. Furthermore, the present technology for the activation of stable C(sp<sup>3</sup>)-O bonds can provide novel carbon circular pathways. Development of a more active Au catalyst that can reduce the number of equivalents of disilanes and broaden the substrate scope is currently underway in our laboratory.

## ■ ASSOCIATED CONTENT

### Supporting Information

The Supporting Information is available free of charge at <https://pubs.acs.org/doi/10.1021/jacs.2c12311>.

Experimental procedures, characterization of supported Au catalysts, and <sup>1</sup>H NMR and <sup>13</sup>C NMR of the products (PDF)

## ■ AUTHOR INFORMATION

### Corresponding Authors

**Hiroki Miura** – Department of Applied Chemistry for Environment, Graduate School of Urban Environmental Sciences, Tokyo Metropolitan University, Tokyo 192-0397, Japan; Research Center for Hydrogen Energy-Based Society, Tokyo Metropolitan University, Tokyo 192-0397, Japan; Elements Strategy Initiative for Catalysts & Batteries, Kyoto University, Kyoto 615-8520, Japan; [orcid.org/0000-0002-2488-4432](https://orcid.org/0000-0002-2488-4432); Email: [miura-hiroki@tmu.ac.jp](mailto:miura-hiroki@tmu.ac.jp)

**Tetsuya Shishido** – Department of Applied Chemistry for Environment, Graduate School of Urban Environmental Sciences, Tokyo Metropolitan University, Tokyo 192-0397, Japan; Research Center for Hydrogen Energy-Based Society,

Tokyo Metropolitan University, Tokyo 192-0397, Japan; Elements Strategy Initiative for Catalysts & Batteries, Kyoto University, Kyoto 615-8520, Japan; [orcid.org/0000-0002-8475-4226](https://orcid.org/0000-0002-8475-4226); Email: [shishido-tetsuya@tmu.ac.jp](mailto:shishido-tetsuya@tmu.ac.jp)

### Authors

**Masafumi Doi** – Department of Applied Chemistry for Environment, Graduate School of Urban Environmental Sciences, Tokyo Metropolitan University, Tokyo 192-0397, Japan

**Yuki Yasui** – Department of Applied Chemistry for Environment, Graduate School of Urban Environmental Sciences, Tokyo Metropolitan University, Tokyo 192-0397, Japan

**Yosuke Masaki** – Department of Applied Chemistry for Environment, Graduate School of Urban Environmental Sciences, Tokyo Metropolitan University, Tokyo 192-0397, Japan

**Hiddenori Nishio** – Department of Applied Chemistry for Environment, Graduate School of Urban Environmental Sciences, Tokyo Metropolitan University, Tokyo 192-0397, Japan

Complete contact information is available at: <https://pubs.acs.org/doi/10.1021/jacs.2c12311>

### Notes

The authors declare no competing financial interest.

## ■ ACKNOWLEDGMENTS

This study was supported in part by the Program for Element Strategy Initiative for Catalysts and Batteries (ESICB) (Grant JPMXP0112101003), JST FOREST Program (Grant JPMJFR203V), Grants-in-Aid for Scientific Research (B)

(Grant 21H01719), Challenging Research (Exploratory) (Grant 22K18927), and Scientific Research on Innovative Areas (Grant 17H06443) commissioned by MEXT of Japan. H.M. wishes to thank Ono of Tokyo Metropolitan University for providing valuable technical support during the HAADF-TEM observations. H.M. also thanks Masazumi Tamura for his kind supply of a polycarbonatediol.<sup>27</sup>

## REFERENCES

- (1) (a) Mora Rollo, A.; Rollo, A.; Mora, C. The Tree-Lined Path to Carbon Neutrality. *Nat. Rev. Earth Environ.* **2020**, *1*, 332. (b) Wang, F.; Harindintwali, J. D.; Yuan, Z.; Wang, M.; Wang, F.; Li, S.; Yin, Z.; Huang, L.; Fu, Y.; Li, L.; Chang, S. X.; Zhang, L.; Rinklebe, J.; Yuan, Z.; Zhu, Q.; Xiang, L.; Tsang, D. C. W.; Xu, L.; Jiang, X.; Liu, J.; Wei, N.; Kästner, M.; Zou, Y.; Ok, Y. S.; Shen, J.; Peng, D.; Zhang, W.; Barceló, D.; Zhou, Y.; Bai, Z.; Li, B.; Zhang, B.; Wei, K.; Cao, H.; Tan, Z.; Zhao, L.; He, X.; Zheng, J.; Bolan, N.; Liu, X.; Huang, C.; Dietmann, S.; Luo, M.; Sun, N.; Gong, J.; Gong, Y.; Brahushi, F.; Zhang, T.; Xiao, C.; Li, X.; Chen, W.; Jiao, N.; Lehmann, J.; Zhu, Y.-G.; Jin, H.; Schäffer, A.; Tiedje, J. M.; Chen, J. M. Technologies and Perspectives for Achieving Carbon Neutrality. *Innovation* **2021**, *2*, No. 100180. (c) Chen, L.; Msigwa, G.; Yang, M.; Osman, A. I.; Fawzy, S.; Rooney, D. W.; Yap, P.-S. Strategies to Achieve a Carbon Neutral Society: A Review. *Environ. Chem. Lett.* **2022**, *20*, 2277–2310. (d) Fankhauser, S.; Smith, S. M.; Allen, M.; Axelsson, K.; Hale, T.; Hepburn, C.; Kendall, J. M.; Khosla, R.; Lezaun, J.; Mitchell-Larson, E.; Obersteiner, M.; Rajamani, L.; Rickaby, R.; Seddon, N.; Wetzler, T. The Meaning of Net Zero and How to Get It Right. *Nat. Clim. Change* **2022**, *12*, 15–21. (e) Zhang, R.; Hanaoka, T. Cross-Cutting Scenarios and Strategies for Designing Decarbonization Pathways in the Transport Sector toward Carbon Neutrality. *Nat. Commun.* **2022**, *13*, No. 3629.
- (2) (a) Li, B.-J.; Yu, D.-G.; Sun, C.-L.; Shi, Z.-J. Activation of “Inert” Alkenyl/Aryl C–O Bond and Its Application in Cross-Coupling Reactions. *Chem. - Eur. J.* **2011**, *17*, 1728–1759. (b) Cornella, J.; Zarate, C.; Martin, R. Metal-Catalyzed Activation of Ethers via C–O Bond Cleavage: A New Strategy for Molecular Diversity. *Chem. Soc. Rev.* **2014**, *43*, 8081–8097. (c) Tobisu, M.; Chatani, N. Cross-Couplings Using Aryl Ethers via C–O Bond Activation Enabled by Nickel Catalysts. *Acc. Chem. Res.* **2015**, *48*, 1717–1726. (d) Bisz, E.; Szostak, M. Iron-Catalyzed C–O Bond Activation: Opportunity for Sustainable Catalysis. *ChemSusChem* **2017**, *10*, 3964–3981. (e) Boit, T. B.; Bulger, A. S.; Dander, J. E.; Garg, N. K. Activation of C–O and C–N Bonds Using Non-Precious-Metal Catalysis. *ACS Catal.* **2020**, *10*, 12109–12126.
- (3) (a) Miyake, Y.; Uemura, S.; Nishibayashi, Y. Catalytic Propargylic Substitution Reactions. *ChemCatChem* **2009**, *1*, 342–356. (b) Sundararaju, B.; Achard, M.; Bruneau, C. Transition Metal Catalyzed Nucleophilic Allylic Substitution: Activation of Allylic Alcohols via  $\pi$ -Allylic Species. *Chem. Soc. Rev.* **2012**, *41*, 4467–4483. (c) Butt, N. A.; Zhang, W. Transition Metal-Catalyzed Allylic Substitution Reactions with Unactivated Allylic Substrates. *Chem. Soc. Rev.* **2015**, *44*, 7929–7967. (d) Dryzhakov, M.; Richmond, E.; Moran, J. Recent Advances in Direct Catalytic Dehydrative Substitution of Alcohols. *Synthesis* **2016**, *48*, 935–959.
- (4) (a) Grote, R. E.; Jarvo, E. R. Palladium-Catalyzed, One-Pot, Three-Component Synthesis of Homoallylic Amines from Aldehydes, Anisidine, and Allyl Trifluoroacetate. *Org. Lett.* **2009**, *11*, 485–488. (b) Dhakal, B.; Bohé, L.; Crich, D. J. *Org. Chem.* **2017**, *82*, 9263–9269.
- (5) (a) Suga, T.; Ukaji, Y. Nickel-Catalyzed Cross-Electrophile Coupling between Benzyl Alcohols and Aryl Halides Assisted by Titanium Co-Reductant. *Org. Lett.* **2018**, *20*, 7846–7850. (b) Dong, Z.; MacMillan, D. W. C. Metallaphotoredox-Enabled Deoxygenative Arylation of Alcohols. *Nature* **2021**, *598*, 451–456. (c) Li, Z.; Sun, W.; Wang, X.; Li, L.; Zhang, Y.; Li, C. Electrochemically Enabled, Nickel-Catalyzed Dehydroxylative Cross-Coupling of Alcohols with Aryl Halides. *J. Am. Chem. Soc.* **2021**, *143*, 3536–3543. (d) Guo, P.; Wang, K.; Jin, W.-J.; Xie, H.; Qi, L.; Liu, X.-Y.; Shu, X.-Z. Dynamic Kinetic Cross-Electrophile Arylation of Benzyl Alcohols by Nickel Catalysis. *J. Am. Chem. Soc.* **2021**, *143*, 513–523.
- (6) (a) Xue, W.; Oestreich, M. Copper-Catalyzed Decarboxylative Radical Silylation of Redox-Active Aliphatic Carboxylic Acid Derivatives. *Angew. Chem., Int. Ed.* **2017**, *56*, 11649–11652. (b) Bähr, S.; Xue, W.; Oestreich, M. C(Sp<sup>3</sup>)–Si Cross-Coupling. *ACS Catal.* **2019**, *9*, 16–24. (c) Xue, W.; Oestreich, M. Beyond Carbon: Enantioselective and Enantiospecific Reactions with Catalytically Generated Boryl- and Silylcopper Intermediates. *ACS Cent. Sci.* **2020**, *6*, 1070–1081.
- (7) (a) Nakao, Y.; Takeda, M.; Matsumoto, T.; Hiyama, T. Cross-Coupling Reactions through the Intramolecular Activation of Alkyl(Triorgano)Silanes. *Angew. Chem., Int. Ed.* **2010**, *49*, 4447–4450. (b) Franz, A. K.; Wilson, S. O. Organosilicon Molecules with Medicinal Applications. *J. Med. Chem.* **2013**, *56*, 388–405. (c) Nakajima, Y.; Sato, K.; Shimada, S. Development of Nickel Hydrosilylation Catalysts. *Chem. Rec.* **2016**, *16*, 2379–2387. (d) Komiyama, T.; Minami, Y.; Hiyama, T. Recent Progress in the Cross-Coupling Reaction Using Triorganosilyl-Type Reagents. *Synlett* **2017**, *28*, 1873–1884. (e) Torigoe, T.; Ohmura, T.; Sugimoto, M. Utilization of a Trimethylsilyl Group as a Synthetic Equivalent of a Hydroxyl Group via Chemoselective C(Sp<sup>3</sup>)–H Borylation at the Methyl Group on Silicon. *J. Org. Chem.* **2017**, *82*, 2943–2956.
- (8) (a) Attack, T. C.; Lecker, R. M.; Cook, S. P. Iron-Catalyzed Borylation of Alkyl Electrophiles. *J. Am. Chem. Soc.* **2014**, *136*, 9521–9523. (b) Zhou, Y.; Wang, H.; Liu, Y.; Zhao, Y.; Zhang, C.; Qu, J. Iron-Catalyzed Boration of Allylic Esters: An Efficient Approach to Allylic Boronates. *Org. Chem. Front.* **2017**, *4*, 1580–1585. (c) Liu, Y.; Zhou, Y.; Li, D.; Chen, H.; Zhao, J.; Qu, J. Iron-Catalyzed Boration of Cinnamyl Carbonates: A Highly Stereoselective Approach to Cyclopropylboronates. *Org. Chem. Front.* **2019**, *6*, 983–988.
- (9) (a) Inubushi, H.; Kondo, H.; Lesbani, A.; Miyachi, M.; Yamanoi, Y.; Nishihara, H. Direct Synthesis of Alkylsilanes by Platinum-Catalyzed Coupling of Hydrosilanes and Iodoalkanes. *Chem. Commun.* **2013**, *49*, 134–136. (b) Chu, C. K.; Liang, Y.; Fu, G. C. Silicon–Carbon Bond Formation via Nickel-Catalyzed Cross-Coupling of Silicon Nucleophiles with Unactivated Secondary and Tertiary Alkyl Electrophiles. *J. Am. Chem. Soc.* **2016**, *138*, 6404–6407. (c) Scharfbier, J.; Oestreich, M. Copper-Catalyzed Si–B Bond Activation in the Nucleophilic Substitution of Primary Aliphatic Triflates. *Synlett* **2016**, *27*, 1274–1276. (d) Xue, W.; Qu, Z.-W.; Grimme, S.; Oestreich, M. Copper-Catalyzed Cross-Coupling of Silicon Pronucleophiles with Unactivated Alkyl Electrophiles Coupled with Radical Cyclization. *J. Am. Chem. Soc.* **2016**, *138*, 14222–14225. (e) Scharfbier, J.; Hazrati, H.; Irran, E.; Oestreich, M. Copper-Catalyzed Substitution of  $\alpha$ -Triflyloxy Nitriles and Esters with Silicon Nucleophiles under Inversion of the Configuration. *Org. Lett.* **2017**, *19*, 6562–6565. (f) Cui, B.; Jia, S.; Tokunaga, E.; Shibata, N. Defluorosilylation of Fluoroarenes and Fluoroalkanes. *Nat. Commun.* **2018**, *9*, No. 4393. (g) Hazrati, H.; Oestreich, M. Copper-Catalyzed Double C(Sp<sup>3</sup>)–Si Coupling of Geminal Dibromides: Ionic-to-Radical Switch in the Reaction Mechanism. *Org. Lett.* **2018**, *20*, 5367–5369. (h) Xue, W.; Shishido, R.; Oestreich, M. Bench-Stable Stock Solutions of Silicon Grignard Reagents: Application to Iron- and Cobalt-Catalyzed Radical C(Sp<sup>3</sup>)–Si Cross-Coupling Reactions. *Angew. Chem., Int. Ed.* **2018**, *57*, 12141–12145. (i) Mallick, S.; Würthwein, E.-U.; Studer, A. Synthesis of Alkyl Silanes via Reaction of Unactivated Alkyl Chlorides and Triflates with Silyl Lithium Reagents. *Org. Lett.* **2020**, *22*, 6568–6572. (j) Scharfbier, J.; Gross, B. M.; Oestreich, M. Stereospecific and Chemoselective Copper-Catalyzed Deaminative Silylation of Benzylic Ammonium Triflates. *Angew. Chem., Int. Ed.* **2020**, *59*, 1577–1580.
- (10) (a) Murakami, K.; Yorimitsu, H.; Oshima, K. Zinc-Catalyzed Nucleophilic Substitution Reaction of Chlorosilanes with Organomagnesium Reagents. *J. Org. Chem.* **2009**, *74*, 1415–1417. (b) Cinderella, A. P.; Vulovic, B.; Watson, D. A. Palladium-Catalyzed Cross-Coupling of Silyl Electrophiles with Alkylzinc Halides: A Silyl-Negishi Reaction. *J. Am. Chem. Soc.* **2017**, *139*, 7741–7744. (c) Vulovic, B.



Cinderella, A. P.; Watson, D. A. Palladium-Catalyzed Cross-Coupling of Monochlorosilanes and Grignard Reagents. *ACS Catal.* **2017**, *7*, 8113–8117.

(11) (a) Duan, J.; Wang, Y.; Qi, L.; Guo, P.; Pang, X.; Shu, X.-Z. Nickel-Catalyzed Cross-Electrophile  $C(Sp^3)$ –Si Coupling of Unactivated Alkyl Bromides with Vinyl Chlorosilanes. *Org. Lett.* **2021**, *23*, 7855–7859. (b) Xing, M.; Cui, H.; Zhang, C. Nickel-Catalyzed Reductive Cross-Coupling of Alkyl Bromides and Chlorosilanes. *Org. Lett.* **2021**, *23*, 7645–7649. (c) Zhang, L.; Oestreich, M. Nickel-Catalyzed, Reductive  $C(Sp^3)$ –Si Cross-Coupling of  $\alpha$ -Cyano Alkyl Electrophiles and Chlorosilanes. *Angew. Chem., Int. Ed.* **2021**, *60*, 18587–18590. (d) Pang, X.; Su, P.-F.; Shu, X.-Z. Reductive Cross-Coupling of Unreactive Electrophiles. *Acc. Chem. Res.* **2022**, *55*, 2491–2509.

(12) (a) Tsuji, Y.; Kajita, S.; Isobe, S.; Funato, M. Palladium-Catalyzed Silylation of Allylic Acetates with Hexamethyldisilane or (Trimethylsilyl)tributylstannane. *J. Org. Chem.* **1993**, *58*, 3607–3608. (b) Moser, R.; Nishikata, T.; Lipshutz, B. H. Pd-Catalyzed Synthesis of Allylic Silanes from Allylic Ethers. *Org. Lett.* **2010**, *12*, 28–31. (c) Takeda, M.; Shintani, R.; Hayashi, T. Enantioselective Synthesis of  $\alpha$ -Tri- and  $\alpha$ -Tetrasubstituted Allylsilanes by Copper-Catalyzed Asymmetric Allylic Substitution of Allyl Phosphates with Silylboronates. *J. Org. Chem.* **2013**, *78*, 5007–5017. (d) Zarate, C.; Martin, R. A Mild Ni/Cu-Catalyzed Silylation via C–O Cleavage. *J. Am. Chem. Soc.* **2014**, *136*, 2236–2239. (e) Zhang, T.; Zheng, S.; Kobayashi, T.; Maekawa, H. Regioselective Silylations of Propargyl and Allyl Pivalates through Ca-Promoted Reductive  $C(Sp^3)$ –O Bond Cleavage. *Org. Lett.* **2021**, *23*, 7129–7133.

(13) (a) Kjellgren, J.; Sundén, H.; Szabó, K. J. Palladium Pincer Complex-Catalyzed Trimethyltin Substitution of Functionalized Propargylic Substrates. An Efficient Route to Propargyl- and Allenyl-Stannanes. *J. Am. Chem. Soc.* **2004**, *126*, 474–475. (b) Ohmiya, H.; Ito, H.; Sawamura, M. General and Functional Group-Tolerable Approach to Allenylsilanes by Rhodium-Catalyzed Coupling between Propargylic Carbonates and a Silylboronate. *Org. Lett.* **2009**, *11*, 5618–5620. (c) Vyas, D. J.; Hazra, C. K.; Oestreich, M. Copper(I)-Catalyzed Regioselective Propargylic Substitution Involving Si–B Bond Activation. *Org. Lett.* **2011**, *13*, 4462–4465. (d) Liu, Z.-L.; Yang, C.; Xue, Q.-Y.; Zhao, M.; Shan, C.-C.; Xu, Y.-H.; Loh, T.-P. Copper-Catalyzed Asymmetric Silylation of Propargyl Dichlorides: Access to Enantioenriched Functionalized Allenylsilanes. *Angew. Chem., Int. Ed.* **2019**, *58*, 16538–16542. (e) Guo, K.; Kleij, A. W. Cu-Catalyzed Synthesis of Tetrasubstituted 2,3-Allenols through Decarboxylative Silylation of Alkyne-Substituted Cyclic Carbonates. *Org. Lett.* **2020**, *22*, 3942–3945.

(14) (a) Anastas, P. T.; Allen, D. T. Twenty-Five Years of Green Chemistry and Green Engineering: The End of the Beginning. *ACS Sustainable Chem. Eng.* **2016**, *4*, 5820. (b) Liu, L.; Corma, A. Metal Catalysts for Heterogeneous Catalysis: From Single Atoms to Nanoclusters and Nanoparticles. *Chem. Rev.* **2018**, *118*, 4981–5079.

(15) (a) Lykakis, I. N.; Psyllaki, A.; Stratakis, M. Oxidative Cycloaddition of 1,1,3,3-Tetramethyldisiloxane to Alkynes Catalyzed by Supported Gold Nanoparticles. *J. Am. Chem. Soc.* **2011**, *133*, 10426–10429. (b) Stratakis, M.; Garcia, H. Catalysis by Supported Gold Nanoparticles: Beyond Aerobic Oxidative Processes. *Chem. Rev.* **2012**, *112*, 4469–4506. (c) Stratakis, M.; Garcia, H. Catalysis by Supported Gold Nanoparticles: Beyond Aerobic Oxidative Processes. *Chem. Rev.* **2012**, *112*, 4469–4506. (d) Gryparis, C.; Kidonakis, M.; Stratakis, M. Supported Gold Nanoparticle-Catalyzed Cis-Selective Disilylation of Terminal Alkynes by  $\sigma$  Disilanes. *Org. Lett.* **2013**, *15*, 6038–6041. (e) Kidonakis, M.; Stratakis, M. Ligandless Regioselective Hydrosilylation of Allenes Catalyzed by Gold Nanoparticles. *Org. Lett.* **2015**, *17*, 4538–4541. (f) Kidonakis, M.; Mullaj, A.; Stratakis, M. Reaction of Aromatic Carbonyl Compounds with Silylborane Catalyzed by Au Nanoparticles: Silylative Pinacol-Type Reductive Dimerization via a Radical Pathway. *J. Org. Chem.* **2018**, *83*, 15553–15557. (g) Stratakis, M.; Lykakis, I. N. Nanogold(0)-Catalyzed Addition of Heteroelement  $\sigma$  Linkages to Functional Groups. *Synthesis* **2019**, *51*, 2435–2454. (h) Miura, H.; Hirata, R.;

Tomoya, T.; Shishido, T. Electrophilic  $C(Sp^2)$ –H Silylation by Supported Gold Catalysts. *ChemCatChem* **2021**, *13*, 4705–4713. (i) Miura, H.; Hachiya, Y.; Nishio, H.; Fukuta, Y.; Toyomasu, T.; Kobayashi, K.; Masaki, Y.; Shishido, T. Practical Synthesis of Allyl, Allenyl, and Benzyl Boronates through  $S_N1'$ -Type Borylation under Heterogeneous Gold Catalysis. *ACS Catal.* **2021**, *11*, 758–766. (j) Miura, H.; Toyomasu, T.; Nishio, H.; Shishido, T. Gold-Catalyzed Thioetherification of Allyl, Benzyl, and Propargyl Phosphates. *Catal. Sci. Technol.* **2022**, *12*, 1109–1116.

(16) (a) Kaneda, K.; Mitsudome, T. Metal-Support Cooperative Catalysts for Environmentally Benign Molecular Transformations. *Chem. Rev.* **2017**, *17*, 4–26. (b) Sankar, M.; He, Q.; Engel, R. V.; Sainna, M. A.; Logsdail, A. J.; Roldan, A.; Willock, D. J.; Agarwal, N.; Kiely, C. J.; Hutchings, G. J. Role of the Support in Gold-Containing Nanoparticles as Heterogeneous Catalysts. *Chem. Rev.* **2020**, *120*, 3890–3938.

(17) (a) Geyer, R.; Jambeck, J. R.; Law, K. L. Production, Use, and Fate of All Plastics Ever Made. *Sci. Adv.* **2017**, *3*, No. e1700782. (b) Ragaert, K.; Delva, L.; Van Geem, K. Mechanical and Chemical Recycling of Solid Plastic Waste. *Waste Manage.* **2017**, *69*, 24–58. (c) Singh, N.; Hui, D.; Singh, R.; Ahuja, I. P. S.; Feo, L.; Fraternali, F. Recycling of Plastic Solid Waste: A State of Art Review and Future Applications. *Composites, Part B* **2017**, *115*, 409–422.

(18) (a) Yoshida, S.; Hiraga, K.; Takehana, T.; Taniguchi, I.; Yamaji, H.; Maeda, Y.; Toyohara, K.; Miyamoto, K.; Kimura, Y.; Oda, K. A Bacterium That Degrades and Assimilates Poly(Ethylene Terephthalate). *Science* **2016**, *351*, 1196–1199. (b) Abel, B. A.; Snyder, R. L.; Coates, G. W. Chemically Recyclable Thermoplastics from Reversible-Deactivation Polymerization of Cyclic Acetals. *Science* **2021**, *373*, 783–789. (c) Weckhuysen, B. M. Creating Value from Plastic Waste. *Science* **2020**, *370*, 400–401. (d) Zhou, H.; Ren, Y.; Li, Z.; Xu, M.; Wang, Y.; Ge, R.; Kong, X.; Zheng, L.; Duan, H. Electrocatalytic Upcycling of Polyethylene Terephthalate to Commodity Chemicals and  $H_2$  Fuel. *Nat. Commun.* **2021**, *12*, No. 4679. (e) Plastic Upcycling. *Nat. Catal.* **2019**, *2*, 945–946 DOI: 10.1038/s41929-019-0391-7. (f) Chu, M.; Liu, Y.; Lou, X.; Zhang, Q.; Chen, J. Rational Design of Chemical Catalysis for Plastic Recycling. *ACS Catal.* **2022**, *12*, 4659–4679. (g) Payne, J.; Jones, M. D. The Chemical Recycling of Polyesters for a Circular Plastics Economy: Challenges and Emerging Opportunities. *ChemSusChem* **2021**, *14*, 4041–4070. (h) Cornwall, W. The Plastic Eaters. *Science* **2021**, *373*, 36–39. (i) Celik, G.; Kennedy, R. M.; Hackler, R. A.; Ferrandon, M.; Tennakoon, A.; Patnaik, S.; LaPointe, A. M.; Ammal, S. C.; Heyden, A.; Perras, F. A.; Pruski, M.; Scott, S. L.; Poeppelmeier, K. R.; Sadow, A. D.; Delferro, M. Upcycling Single-Use Polyethylene into High-Quality Liquid Products. *ACS Cent. Sci.* **2019**, *5*, 1795–1803.

(19) (a) Delle Chiaie, K. R.; McMahon, F. R.; Williams, E. J.; Price, M. J.; Dove, A. P. Dual-Catalytic Depolymerization of Polyethylene Terephthalate (PET). *Polym. Chem.* **2020**, *11*, 1450–1453. (b) Tanaka, S.; Sato, J.; Nakajima, Y. Capturing Ethylene Glycol with Dimethyl Carbonate towards Depolymerisation of Polyethylene Terephthalate at Ambient Temperature. *Green Chem.* **2021**, *23*, 9412–9416. (c) Payne, J. M.; Kociok-Köhn, G.; Emanuelsson, E. A. C.; Jones, M. D. Zn(II)- and Mg(II)-Complexes of a Tridentate {ONN} Ligand: Application to Poly(Lactic Acid) Production and Chemical Upcycling of Polyesters. *Macromolecules* **2021**, *54*, 8453–8469. (d) Abe, R.; Komine, N.; Nomura, K.; Hirano, M. La(III)-Catalysed Degradation of Polyesters to Monomers via Transesterifications. *Chem. Commun.* **2022**, *58*, 8141–8144.

(20) (a) Monsigny, L.; Berthet, J.-C.; Cantat, T. Depolymerization of Waste Plastics to Monomers and Chemicals Using a Hydrosilylation Strategy Facilitated by Brookhart's Iridium(III) Catalyst. *ACS Sustainable Chem. Eng.* **2018**, *6*, 10481–10488. (b) Kumar, A.; von Wolff, N.; Rauch, M.; Zou, Y.-Q.; Shmul, G.; Ben-David, Y.; Leitun, G.; Avram, L.; Milstein, D. Hydrogenative Depolymerization of Nylons. *J. Am. Chem. Soc.* **2020**, *142*, 14267–14275. (c) Kratish, Y.; Li, J.; Liu, S.; Gao, Y.; Marks, T. J. Polyethylene Terephthalate Deconstruction Catalyzed by a Carbon-Supported Single-Site Molybdenum-Dioxo Complex. *Angew. Chem., Int. Ed.* **2020**, *59*,

19857–19861. (d) Ghosh, P.; Jacobi von Wangelin, A. Manganese-Catalyzed Hydroborations with Broad Scope. *Angew. Chem., Int. Ed.* **2021**, *60*, 16035–16043. (e) Fernandes, A. C. Reductive Depolymerization of Plastic Waste Catalyzed by  $\text{Zn}(\text{OAc})_2 \cdot 2\text{H}_2\text{O}$ . *ChemSusChem* **2021**, *14*, 4228–4233. (f) Kratish, Y.; Marks, T. J. Efficient Polyester Hydrogenolytic Deconstruction via Tandem Catalysis. *Angew. Chem., Int. Ed.* **2022**, *61*, No. e202112576.

(21) (a) Vasilikogiannaki, E.; Louka, A.; Stratakis, M. Gold-Nanoparticle-Catalyzed Silaboration of Oxetanes and Unactivated Epoxides. *Organometallics* **2016**, *35*, 3895–3902. (b) Li, H.; Guo, H.; Li, Z.; Wu, C.; Li, J.; Zhao, C.; Guo, S.; Ding, Y.; He, W.; Li, Y. Silylation Reactions on Nanoporous Gold via Homolytic Si–H Activation of Silanes. *Chem. Sci.* **2018**, *9*, 4808–4813.

(22) Yu, X.; Lübbesmeier, M.; Studer, A. Oligosilanes as Silyl Radical Precursors through Oxidative Si–Si Bond Cleavage Using Redox Catalysis. *Angew. Chem., Int. Ed.* **2021**, *60*, 675–679.

(23) Baudler, A.; Schmidt, I.; Langner, M.; Greiner, A.; Schröder, U. Does It Have to Be Carbon? Metal Anodes in Microbial Fuel Cells and Related Bioelectrochemical Systems. *Energy Environ. Sci.* **2015**, *8*, 2048–2055.

(24) (a) Hutchings, G. J.; Hall, M. S.; Carley, A. F.; Landon, P.; Solsona, B. E.; Kiely, C. J.; Herzing, A.; Makkee, M.; Moulijn, J. A.; Overweg, A.; Fierro-Gonzalez, J. C.; Guzman, J.; Gates, B. C. Role of Gold Cations in the Oxidation of Carbon Monoxide Catalyzed by Iron Oxide-Supported Gold. *J. Catal.* **2006**, *242*, 71–81. (b) Comotti, M.; Li, W.-C.; Spliethoff, B.; Schüth, F. Support Effect in High Activity Gold Catalysts for CO Oxidation. *J. Am. Chem. Soc.* **2006**, *128*, 917–924. (c) Longo, A.; Liotta, L. F.; Pantaleo, G.; Giannici, F.; Venezia, A. M.; Martorana, A. Structure of the Metal–Support Interface and Oxidation State of Gold Nanoparticles Supported on Ceria. *J. Phys. Chem. C* **2012**, *116*, 2960–2966. (d) Fujitani, T.; Nakamura, I.; Takahashi, A.  $\text{H}_2\text{O}$  Dissociation at the Perimeter Interface between Gold Nanoparticles and  $\text{TiO}_2$  Is Crucial for Oxidation of CO. *ACS Catal.* **2020**, *10*, 2517–2521. (e) Nakayama, A.; Sodenaga, R.; Gangarajula, Y.; Taketoshi, A.; Murayama, T.; Honma, T.; Sakaguchi, N.; Shimada, T.; Takagi, S.; Haruta, M.; Qiao, B.; Wang, J.; Ishida, T. Enhancement Effect of Strong Metal-Support Interaction (SMSI) on the Catalytic Activity of Substituted-Hydroxyapatite Supported Au Clusters. *J. Catal.* **2022**, *410*, 194–205.

(25) (a) Barton, D. H. R.; McCombie, S. W. A new method for the deoxygenation of secondary alcohols. *J. Chem. Soc., Perkin Trans. 1* **1975**, 1574–1585. (b) Liu, Z.-Y.; Cook, S. P. Interrupting the Barton–McCombie Reaction: Aqueous Deoxygenative Trifluoromethylation of *O*-Alkyl Thiocarbonates. *Org. Lett.* **2021**, *23*, 808–813.

(26) Zhang, Y.; Chen, J.; Huang, H. Radical Brook Rearrangements: Concept and Recent Developments. *Angew. Chem., Int. Ed.* **2022**, *61*, No. e202205671.

(27) (a) Gu, Y.; Matsuda, K.; Nakayama, A.; Tamura, M.; Nakagawa, Y.; Tomishige, K. Direct Synthesis of Alternating Polycarbonates from  $\text{CO}_2$  and Diols by Using a Catalyst System of  $\text{CeO}_2$  and 2-Furionitrile. *ACS Sustainable Chem. Eng.* **2019**, *7*, 6304–6315. (b) Gu, Y.; Tamura, M.; Nakagawa, Y.; Nakao, K.; Suzuki, K.; Tomishige, K. Direct Synthesis of Polycarbonate Diols from Atmospheric Flow  $\text{CO}_2$  and Diols without Using Dehydrating Agents. *Green Chem.* **2021**, *23*, 5786–5796.